

## Optical Temperature Measurement Method for Glowing Microcomponents

M. Shpak · P. Kärhä · M. Ojanen · E. Ikonen ·  
M. Heinonen

Received: 8 March 2010 / Accepted: 22 September 2010 / Published online: 8 October 2010  
© Springer Science+Business Media, LLC 2010

**Abstract** A measurement method and measurement results for the temperature of miniature microbridge emitters integrated on silicon are presented. First, the extinction coefficient of highly doped silicon was measured at high temperatures: a piece of a silicon-on-insulator wafer was heated to several temperatures in a high-temperature furnace, and the emitted spectra were measured using a spectroradiometer with focusing optics. The optical behavior of the sample was modeled with Fresnel equations. The extinction coefficient of silicon was obtained from the model, because other optical properties, the dimensions, and the temperature of the structure were known. An emissivity model was then developed and adapted for the microbridge with the known extinction coefficient values, which allows the temperature to be determined from the measured spectrum. We can now measure optically the temperatures of the microbridges of dimensions  $400 \times 25 \times 4 \mu\text{m}^3$  in the temperature range  $600^\circ\text{C}$  to  $1200^\circ\text{C}$  with an uncertainty of  $100^\circ\text{C}$ .

**Keywords** Emissivity · High temperatures · Microbridge · Refractive index · Silicon

### 1 Introduction

Optical temperature measurement of small components possesses many challenges. To estimate the temperature of the component from the shape of the radiation spectrum with Planck's radiation law, a knowledge of the emissivity is needed. Emissivity is

---

M. Shpak (✉) · P. Kärhä · M. Ojanen · E. Ikonen  
Metrology Research Institute, Aalto University, P.O. Box 13000, 00076 Aalto, Finland  
e-mail: maksim.shpak@tkk.fi

E. Ikonen · M. Heinonen  
Centre for Metrology and Accreditation, P.O. Box 9, 02151 Espoo, Finland

a function of the geometric surface properties and the refractive index of the material. In the case of silicon (Si), the imaginary part of the refractive index—extinction coefficient—is a strong function of the doping concentration and the temperature. In particular, the extinction coefficient of highly doped silicon (Si++) changes rapidly at temperatures above 700 °C, as the silicon moves from the extrinsic to the intrinsic temperature range. For miniature components, semi-transparency causes light interference effects, which may significantly affect the wavelength dependence of emissivity.

Microbridges are miniature-suspended silicon structures, commonly known for their mechanical properties as cantilevers and actuators. Due to good thermal stability, the temperature of a microbridge protected by silicon dioxide ( $\text{SiO}_2$ ) can be rapidly brought close to the melting point of silicon (1400 °C) by passing an electrical current through the bridge [1]. At these temperatures, the microbridge glows as a filament and can be used as a miniature wideband light source. Microbridges are used as light sources in various spectrophotometric applications, such as gas analysis systems [2,3]. Several studies have investigated microbridges at high temperatures, but many of them relied on the greybody assumption [4–8].

In this study, we present a measurement method for optical temperature measurements of microbridges. We first determined the extinction coefficient of highly doped silicon by observing the behavior of a silicon-on-insulator (SOI) wafer sample at several known temperatures. The sample was heated in a high-temperature furnace, and its radiance was measured with a spectroradiometer with focusing optics in the wavelength range from 400 nm to 2500 nm. The temperature of the sample was measured with a calibrated thermocouple. The emissivity was determined with help of Planck's radiation law and the known temperature. A thin-film model based on Fresnel equations was constructed to describe the emissivity of the multilayer sample structure. The spectral extinction coefficient of silicon was determined using an eight-degree polynomial fit.

The emissivity model was then applied in a temperature measurement of a microbridge. The spectral radiance of a glowing microbridge was measured with a spectroradiometer with microscope optics. The temperature was determined using Planck's radiation law combined with the modeled emissivity. The uncertainty of the measurements is approximately 100 °C.

In Sect. 2, we present the model used for deriving the temperature from a measured spectrum. The theory and the measurement setup needed to derive the optical properties of silicon needed to analyze the emissivities of the structures are presented in Sect. 3. Section 4 presents the measurement setup that was used to measure the temperature of the microbridge. All measurement results are given in Sect. 5 and discussed in Sect. 6.

## 2 Determination of Temperature from the Radiation Spectrum

Spectral distribution of the electromagnetic radiation emitted by an object with temperature  $T$  is described by the Planck's radiation law multiplied by the emissivity of the object as

$$S(\lambda, T) = B \varepsilon(\lambda, T) \frac{2hc^2}{\lambda^5} \frac{1}{\exp\left(\frac{hc}{\lambda kT}\right) - 1}, \quad (1)$$

where  $\lambda$  is the wavelength,  $h$  is the Planck constant,  $c$  is the speed of light,  $k$  is the Boltzmann constant,  $\varepsilon$  is the emissivity, and  $B$  is a geometrical factor. The geometrical factor  $B$  depends on the optical geometry of the measurement setup, and remains constant throughout the measurements at different temperatures. By measuring the spectrum, the temperature may be derived by fitting Eq. 1 to the measurement results. The absolute values of the intensity are typically not needed. The temperature can be determined from the shape of the spectrum, provided that the emissivity is known.

### 3 Optical Properties of Silicon

The emissivity of a sample is a function of the refractive indices of the materials used and the geometrical configuration. Although optical properties of silicon have been studied extensively and the fundamental mechanisms of absorption are well known [9–12], there are little data for the behavior of highly doped silicon at high temperatures.

For the real part of the refractive index, we used expressions of Jellison and Modine [11] for wavelengths below  $0.84\text{ }\mu\text{m}$ , and the expression of Li [12] for wavelengths above  $1.2\text{ }\mu\text{m}$ . For the  $0.84\text{ }\mu\text{m}$  to  $1.2\text{ }\mu\text{m}$  wavelength range, a weighted average of both expressions is used, as proposed by Lee et al. [13].

The imaginary part of the refractive index—the extinction coefficient—depends on the absorption processes in silicon, such as the band-to-band transition, free-carrier absorption, and absorption due to lattice vibration [9]. In the spectral range of interest, free-carrier absorption is significant, as it is directly influenced by the doping concentration, and it exhibits complicated behavior at temperatures near and above the intrinsic temperature. Studies of the extinction coefficient of doped silicon are mostly confined to temperatures below  $800\text{ }^\circ\text{C}$ . Disagreement between the proposed empirical models increases with extrapolation to higher temperatures and higher doping levels. The extinction coefficient was therefore determined experimentally, by measuring and modeling the emissivity of a SOI wafer at high temperatures, and fitting the extinction coefficient in the model with an eighth-degree polynomial.

For silicon dioxide, the real part of the refractive index was taken from Malitson [14], and the extinction coefficient was assumed to be negligible.

#### 3.1 Thin-Film Model

For thin, multi-layered structures, effects of semi-transparency and light interference in the layers have to be taken into account. Emissivity can be expressed as a function of reflectivity  $\rho$  and transmissivity  $\tau$ , as

$$\varepsilon(\lambda) = 1 - \rho(\lambda) - \tau(\lambda). \quad (2)$$

The total reflection and transmission coefficients of a stack of thin films can be calculated using Fresnel equations [15]. Figure 1 illustrates the propagation of light waves

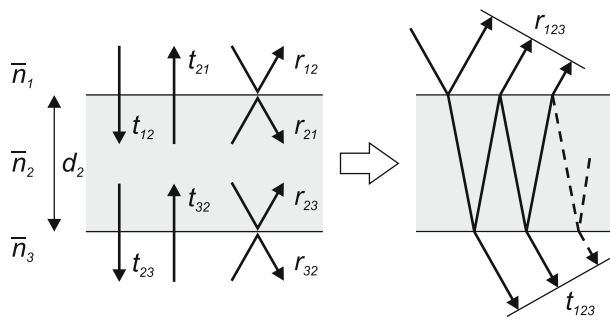


**Fig. 1** Light propagation in thin layers. For abbreviations, see text

in thin layers. For one thin-film sample, the amplitude coefficients for the coherent transmission  $t_{123}$  and reflection  $r_{123}$  are sums of geometric series,

$$t_{123} = \frac{t_{12}t_{23}e^{i\beta_2}}{1 - r_{21}r_{23}e^{2i\beta_2}}, \quad (3)$$

$$r_{123} = r_{12} + \frac{t_{12}t_{23}r_{23}e^{2i\beta_2}}{1 - r_{21}r_{23}e^{2i\beta_2}}, \quad (4)$$

where  $t_{mn}$  and  $r_{mn}$  ( $m, n = 1, 2, 3$ ) are the transmission and reflection coefficients for a wave traveling from material  $m$  to material  $n$ . Parameter  $\beta_2$  is defined as

$$\beta_2 = \frac{2\pi}{\lambda}d_2\bar{n}_2 = \frac{2\pi}{\lambda}d_2(n_2 + ik_2), \quad (5)$$

where  $d_2$  is the thickness of the thin film and  $\bar{n}_2$  is the complex index of refraction. The imaginary part of the refractive index  $k_2$  is the extinction coefficient of the material. The transmission and reflection amplitude coefficients  $t_{mn}$  and  $r_{mn}$  are

$$t_{mn} = \frac{2\bar{n}_m}{\bar{n}_m + \bar{n}_n}, \quad (6)$$

and

$$r_{mn} = \frac{\bar{n}_m - \bar{n}_n}{\bar{n}_m + \bar{n}_n}. \quad (7)$$

The polarization indices are omitted here, because normal incidence is assumed. In this way, a system with two interfaces can be treated as a system with only one interface. All information about the wave propagation inside the eliminated layer is contained in the parameters  $t_{123}$  and  $r_{123}$ . The process can be repeated by adding interfaces to the bottom of the stack, and the total transmission and reflection amplitude coefficients for any number of thin films can be calculated. Amplitude coefficients are converted to intensity coefficients, which are needed in Eq. 2, by taking their absolute squared values.

### 3.2 Setup for Measurement Of Emissivity

The SOI wafer used in the measurement consisted of four optical layers: 380  $\mu\text{m}$  Si substrate layer, 200 nm SiO<sub>2</sub> buried oxide layer, 4  $\mu\text{m}$  Si++ device layer, and a 200 nm to 500 nm SiO<sub>2</sub> protective top layer. The thickness of the top layer increases during the measurements due to accelerated oxidation of silicon at high temperatures. The cross section is presented in Fig. 2. The doping concentration of the device layer is  $5 \times 10^{18} \text{ cm}^{-3}$ . The size of the sample was approximately  $4 \times 3 \text{ cm}^2$ . The piece of the wafer was placed vertically in a high-temperature furnace, and its spectral radiance was measured with a spectroradiometer. A photograph of the measurement setup is presented in Fig. 3. The temperature of the sample was measured with a K-type thermocouple from the titanium holder supporting the sample. The spectroradiometer consisted of a double monochromator with focusing telescope optics that measured spectral radiance over a 5 mm diameter spot at the distance of 1 m. The detection was made with a photomultiplier tube in the wavelength range of 400 nm to 850 nm and with a lead-sulfide detector in the range of 850 nm to 2500 nm. The bandwidths were 3 nm and 10 nm for the two ranges, respectively.

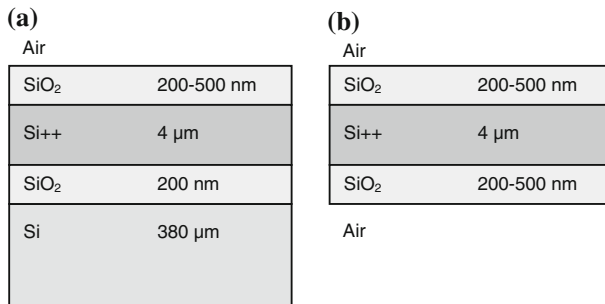


**Fig. 2** Cross-section schematic of (a) the SOI wafer and (b) the microbridge



**Fig. 3** Setup for the measurement of emissivity of SOI wafer

Diffusely reflected radiation originating from the walls of the furnace can increase the apparent emissivity. The diffuse reflectance of the SOI sample was measured at a wavelength of 633 nm and at room temperature to be less than 0.02 %. It was assumed that diffuse reflectance does not increase significantly with temperature. The effect was thus considered insignificant and was not taken into account in the calculations.

The spectroradiometer was calibrated by measuring a blackbody radiator operated at 1300 °C. The telescope was focused on the bottom of the blackbody cavity. Because the calibration setup has exactly the same geometry as the actual measurement setup, the obtained radiance values are absolute and the scaling factor  $B$  of Eq. 1 is equal to one.

## 4 Temperature Measurement of Microbridge

To measure the spectral radiance of the microbridge, the setup described in Sect. 3.2 was modified. The input optics was replaced by a microscope objective with a nominal magnification of ten and an aperture at the image plane limiting the area of the measurement. This allowed focusing at the center of the bridge with a measurement spot diameter of approximately 40  $\mu\text{m}$  at a distance of around 1 cm. The detector for the near-infrared range was replaced with an InGaAs detector, which allowed higher sensitivity, but extended only up to 1700 nm.

The dimensions of the microbridge used in this study were  $400 \times 25 \times 4 \mu\text{m}^3$ . A cross-section schematic of the bridge is presented in Fig. 2b. The width of the bridge is smaller than the diameter of the measurement spot, and this is compensated by fitting the free parameter  $B$  in Eq. 1. The bridge is manufactured on the same wafer as described in Sect. 3.2, and therefore the Si++ layer exhibits the same optical properties. The bridge was heated by passing a DC electrical current through it. The results presented were obtained with a current of 12.0 mA.

The calibration of the setup equipped with microscope optics required a known uniform source, which could be placed at close proximity to the objective. We used an integrating sphere with four 50 W halogen lamps. The objective was focused at the plane of the output port of the sphere, which acted as a Lambertian source. The relative spectral radiance of the sphere was obtained by measuring its irradiance with a calibrated spectroradiometer. The calibration of the spectroradiometer is traceable to the national spectral irradiance scale.

## 5 Results

### 5.1 Extinction Coefficient of Silicon

The measured spectral radiance and spectral emissivity of a SOI wafer sample at 1109 °C are presented in Fig. 4a and b. The dashed line in Fig. 4a represents the radiance of an ideal blackbody at the same temperature. Two interference patterns are evident from the emissivity graph: the slower oscillations at the wavelengths below 1  $\mu\text{m}$  are primarily caused by the interference in the top  $\text{SiO}_2$  layer of the sample. The faster oscillations at wavelengths above 1  $\mu\text{m}$  are primarily caused by the interference in the Si++ layer of the sample.

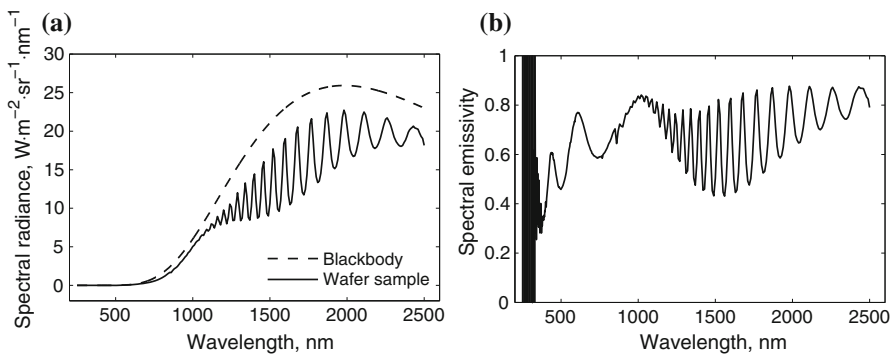
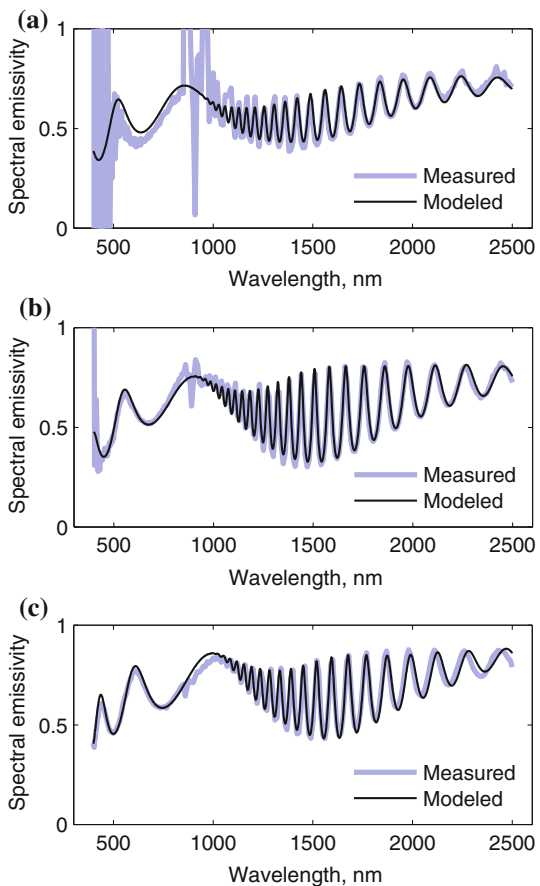


**Fig. 4** (a) Radiance spectrum and (b) emissivity of the SOI wafer sample at 1109 °C

**Fig. 5** Modeled emissivity of the SOI wafer at (a) 719 °C, (b) 914 °C, and (c) 1109 °C



Modeled emissivities of the SOI wafer at temperatures of 719 °C, 914 °C, and 1109 °C are shown in Fig. 5. Thicknesses of the layers, and the coefficients of the eighth-degree polynomial describing the extinction coefficient of Si++, were adjusted

**Fig. 6** Extinction coefficients of highly doped silicon at temperatures of 719 °C, 914 °C, and 1109 °C

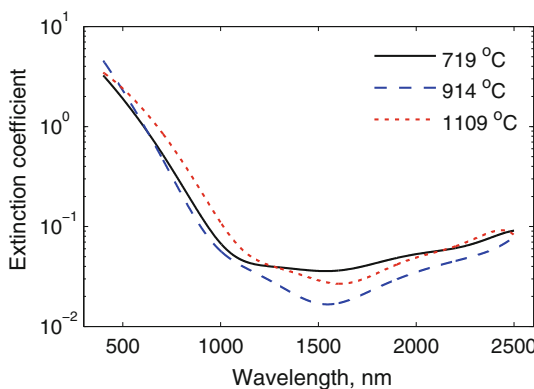


**Table 1** Values of the extinction coefficient of Si++ at three temperatures

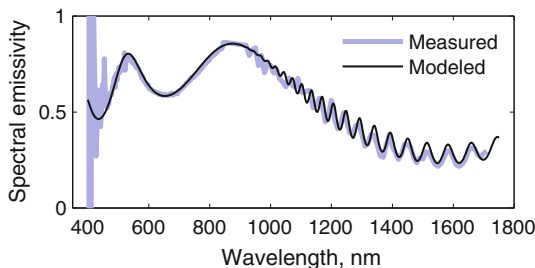
$\lambda$ (nm)	$k$ ( $T = 719$ °C)	$k$ ( $T = 914$ °C)	$k$ ( $T = 1109$ °C)
400	3.250	4.565	3.471
600	1.047	1.089	1.513
800	0.264	0.211	0.460
1000	0.068	0.057	0.110
1200	0.041	0.033	0.045
1400	0.037	0.020	0.033
1600	0.036	0.017	0.027
1800	0.044	0.025	0.034
2000	0.053	0.035	0.049
2200	0.061	0.046	0.063
2400	0.081	0.061	0.089

to obtain an optimal fit. Figure 6 presents the extinction coefficients derived for highly doped silicon at the three temperatures used. Numerical values for the extinction coefficients are presented in Table 1. For the whole wavelength range, the values of the extinction coefficient are higher than the values found in the literature [10, 11] where, however, silicon was measured at lower temperatures.

## 5.2 Microbridge

The microbridge emissivity was modeled with the extinction coefficient determined, using the temperature  $T$  and the scaling variable  $B$  of Eq. 1 as free parameters. Figure 7 presents the measured and modeled spectral emissivities of the microbridge. The best fit was achieved at  $T = 940$  °C. The measurement uncertainty was estimated to be 100 °C. The value is in agreement with a contact measurement using a microthermocouple [16].

**Fig. 7** Measured and modeled spectral emissivities of the microbridge at 940 °C



## 6 Discussion

In this study, we have presented a method for optical temperature measurement of miniature components. The greybody assumption cannot be used due to interference and strong wavelength dependence of the emissivity. For doped silicon in particular, as the temperatures approach levels where carrier conditions shift from extrinsic to intrinsic, the rapid changes in the extinction coefficient result in changes of absorptivity which in turn affects the emissivity. We have successfully utilized measured interference patterns caused by the multi-layered structure of an SOI wafer to estimate the spectral extinction coefficient. With the model for the emissivity of multi-layered structures, relative spectral measurements can be used to derive the temperature.

**Acknowledgments** The authors thank Dr. Lauri Sainiemi and Prof. Sami Franssila for the wafer samples and microbridges used in the measurements, and Dr. Thua Weckström for help in measurement arrangements for the emissivity of silicon. Erkki Ikonen acknowledges Grant No. 129971 from the Academy of Finland.

## References

1. L. Sainiemi, K. Grigoras, I. Kassamakov, K. Hanhijärvi, J. Aaltonen, J. Fan, V. Saarela, E. Hæggström, S. Franssila, *Sens. Actuators A* **149**, 305 (2009)
2. M. Blomberg, O. Rusanen, K. Keranen, A. Lehto, A Silicon Microsystem—Miniatirised Infrared Spectrometer, in *Proceedings of Transducers '97, 9th International Conference on Solid State Sensors and Actuators*, vol. 2 (IEEE, 1997), pp. 1257–1258
3. T. Corman, E. Kälvesten, M. Huiku, K. Weckström, P.T. Meriläinen, G. Stemme, *J. Microelectromech. Syst.* **9**, 509 (2000)
4. J. Tu, D. Howard, S.D. Collins, R.L. Smith, *Appl. Opt.* **42**, 2388 (2003)
5. P. Fürjes, Z. Vizváry, M. Ádám, A. Morrissey, C. Dücső, I. Bársóny, *Sens. Actuators A* **99**, 98 (2002)
6. H. Yuasa, S. Ohya, S. Karasawa, K. Akimoto, S. Kodato, K. Takahashi, Single crystal silicon micromachined pulsed infrared light source, in *Proceedings of Transducers '97, 9th International Conference on Solid State Sensors and Actuators*, vol. 2 (IEEE, 1997), pp. 1271–1274
7. J. Lee, W.P. King, *Sens. Actuators A* **136**, 291 (2007)
8. C.H. Mastrangelo, J.H. Yeh, R.S. Muller, *IEEE Trans. Electron Devices Lett.* **39**, 1363 (1992)
9. T. Satō, *Jpn. J. Appl. Phys.* **6**, 339 (1967)
10. P.J. Timans, *J. Appl. Phys.* **74**, 6353 (1993)
11. G.E. Jellison Jr., F.A. Modine, *J. Appl. Phys.* **76**, 3758 (1994)
12. H.H. Li, *J. Phys. Chem. Ref. Data* **9**, 561 (1980)
13. B.J. Lee, Z.M. Zhang, E.A. Early, D.P. DeWitt, B.K. Tsai, *J. Thermophys. Heat Transf.* **19**, 558 (2005)
14. I.H. Malitson, *J. Opt. Soc. Am.* **55**, 1205 (1965)
15. M. Born, E. Wolf, *Principles of Optics* (Cambridge University Press, Cambridge, 1999)
16. M. Shpak, L. Sainiemi, M. Ojanen, P. Kärhä, M. Heinonen, S. Franssila, E. Ikonen, *Appl. Opt.* **49**, 1489 (2010)